



Identifiability of UHE Gamma-ray Air Showers by Neural-Network-Analysis

Y. WADA¹, N. INOUE¹, K. MIYAZAWA¹ AND H. P. VANKOV²

¹Graduate School of Science and Engineering, Saitama University, Saitama 338-8570, Japan

²Institute for Nuclear Research and Nuclear Energy, Bulgaria Academy, Sofia, Bulgaria

wada@crsgml.crinoue.phy.saitama-u.ac.jp

Abstract: The chemical composition of Ultra-High-Energy (UHE) cosmic rays is one of unsolved questions, and its study will provide us for the information on the origin and the acceleration mechanism of UHE cosmic rays. Especially, a detection of UHE gamma-rays by hybrid experiments, e.g. Auger and Telescope array experiments, will be a key to solve these questions. The characteristics of UHE gamma-ray showers have been studied on lateral and longitudinal structure by AIRES and our own simulation code, so far. There are differences in a slope of lateral distribution (η) and a depth of shower maximum (X_{\max}) between gamma-ray and proton induced showers because UHE gamma-ray showers are affected by the LPM effect and the geomagnetic cascading process in an energy region of $> 10^{19.5}$ eV. Different features between gamma-ray and proton showers are pointed out from the simulation study and an identifiability of gamma-ray showers from proton ones is also discussed by the method of Neural-Network-Analysis.

Introduction

In an energy spectrum of $> 10^{19}$ eV, the GZK cutoff [1] [2] has been predicted to be few cosmic ray flux above 10^{20} eV. However, AGASA had observed 11 events with energies well beyond 10^{20} eV [3]. There are several acceleration models to produce UHE gamma-rays and neutrinos with such a huge energy. Z-burst model predicts that UHE gamma-rays are produced as secondary particles through an interaction between UHE neutrino and cosmic neutrino background. GZK gamma-rays are also expected as a secondary component in GZK process. As the top-down scenario, the decay process of Super Heavy Relic, topological defects, i.e. cosmic string, monopole, etc., are candidates of UHE cosmic ray origin.

Air showers initiated by UHE gamma-rays have characteristic profiles in comparison with hadronic showers. An influence of the LPM effect [4] [5] on shower structures leads to a significant elongation of electromagnetic cascading and a large fluctuation of shower developments at an energy region above $10^{19.5}$ eV. On the other hand, once electron-positron pair is produced in UHE gamma-ray interaction with the geomagnetic field away from the

Earth's surface, it initiates an electromagnetic cascading before entering the atmosphere [6]. As a result, an energy of "primary gamma-ray" is shared by a bunch of lower energy "secondary gamma-rays". Therefore, an influence of the LPM effect on subsequent showers is significantly weakened in the atmosphere. An effect of the geomagnetic cascading on shower structures strongly depends on arrival direction and gamma-ray energy above $10^{19.5}$ eV [7]. In the present work, both a slope of lateral distribution (η) and a depth of shower maximum (X_{\max}) are used as observables to estimate for an identifiability of UHE gamma-ray showers from proton ones.

Simulation

The atmospheric air shower simulation has been carried out by AIRES code (Ver.2.6.0) [8] for primary proton and gamma-ray showers. Individual longitudinal and lateral structure were fitted by the Gaisser-Hillas formula with 3 parameters¹, and by

$$1. N(x) = a_1 \left(\frac{x}{a_2}\right)^{a_2 \times a_3} \times \exp[(a_2 - x)a_3]$$

the modified NKG function with 2 parameters², respectively. Here, a_2 was defined as a slope of lateral distribution (η) in the following discussion. Atmospheric showers of proton and gamma-ray primaries have been generated in an energy region of 10^{17} eV- 10^{21} eV with $\Delta\log(\text{energy})=0.1$ step and zenith angles of 0, 20, 30, 45, 60, 75°. 100 events for each combination of an energy and a zenith angle were simulated, and fitted parameters of lateral and longitudinal structure were accumulated in a library. To simulate showers initiated by UHE gamma-rays, we calculated the geomagnetic cascading starting with a single UHE gamma-ray far away from the Earth's surface down to the top of the atmosphere by own simulation code (the location in Utah TA site was assumed in this calculation). Secondary particles that reached the top of the atmosphere were set as an input component for the calculation of atmospheric shower. Atmospheric gamma-ray shower was constructed as a superposition of lower energy gamma-ray sub-showers which were recorded in a library mentioned above.

Results and Discussion

Characteristics of UHE gamma-ray shower structure

Figure 1 (top) shows X_{max} distributions for proton showers and gamma-ray showers with the geomagnetic cascading process "ON". Primary energies above $10^{19.6}$ eV were sampled from a power law energy spectrum with an index of -2.7. A zenith angle of 45° was assumed and an azimuthal angle was assigned randomly in 0° -360°. When the geomagnetic cascading process is taken into account as a reasonable assumption, atmospheric gamma-ray showers tend to have smaller X_{max} with a smaller fluctuation. Therefore X_{max} distribution of gamma-ray showers approaches near to a region of proton showers and partly overlapped each other. A longer tail in X_{max} distribution of gamma-ray showers could be found. It consists of gamma-ray showers affected by the LPM effect, being superior to the geomagnetic cascading process. Figure 1 (bottom) shows η distributions for proton and gamma-ray showers too. The effects of LPM and geomagnetic cascading process also

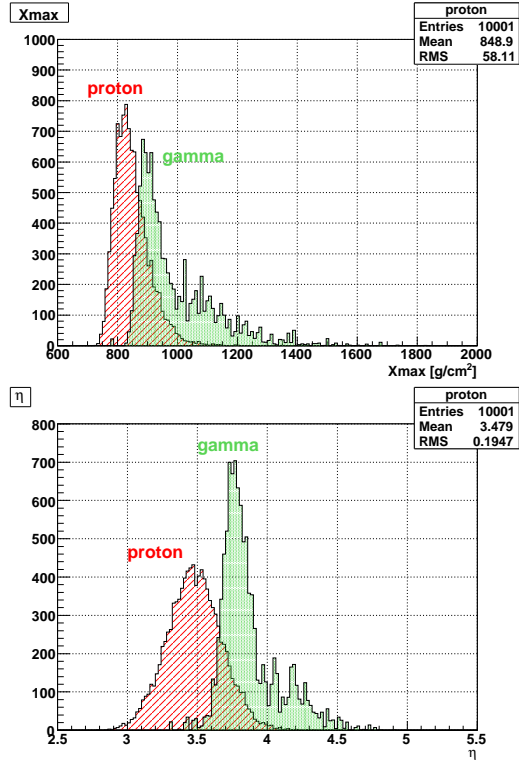


Figure 1: Distributions of X_{max} (top) and η (bottom) for proton and gamma-ray showers of $E > 10^{19.6}$ eV and 45° with the geomagnetic cascading process "ON".

contribute to gamma-ray showers, just as the case of X_{max} distribution.

Neural-Network-Analysis

An identifiability of gamma-ray/proton showers has been studied with the method of Neural-Network-Analysis(NNA). The used network consists of the input, middle and output layer. Three parameters of longitudinal structure, two parameters of lateral structure, a primary energy, a zenith and an azimuthal angle were given into the first layer. Firstly, the network studied on longitudinal and lateral features of simulated proton and gamma-ray showers(10000 events each) with ener-

$$2. N(R) = a_1 \left(\frac{R}{R_m}\right)^{-1.2} \left(1 + \frac{R}{R_m}\right)^{-(a_2-1.2)} \times \left(1 + \left(\frac{R}{1\text{km}}\right)^2\right)^{-0.6}$$

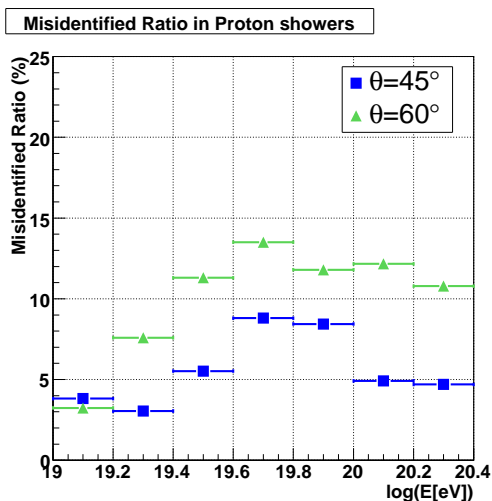


Figure 2: Misidentified ratios of proton showers as a function of primary energy for zenith angles of 45° and 60° .

gies sampled with a power law of -2.7 and a zenith angle of 45° , in order to quantify the combination weights among the layers, by the back propagation method. A set of convergent weights was applied for event identification test. Other datasets of proton and gamma-ray showers (10000 events each) have been tested by NN algorithm and resulting output values from the last layer were evaluated to estimate for a degree of reality of identification. Output values are in a range of 0.0-1.0. Events with 0.0 and 1.0 show the most likely gamma-ray and proton shower candidates, respectively, and an intermediate value shows a degree of uncertainty of particle identification.

When an output of 0.5 is assumed as a judging standard value for an identification between proton and gamma-ray shower, a few proton events with <0.5 and gamma-ray events with >0.5 could be seen as misidentified fake events. A correct answer ratio of tested proton and gamma-ray showers was 97.2% from this calculation.

To examine UHE gamma-ray flux or an assessed reliability of a flux limit, a study of misidentified ratio of proton showers is essentially important. Figure 2 shows misidentified ratios of proton showers with zenith angles of 45° and 60° . Both misidentified ratios of proton showers increase quickly upto $10^{19.8}$ eV, and then they be-

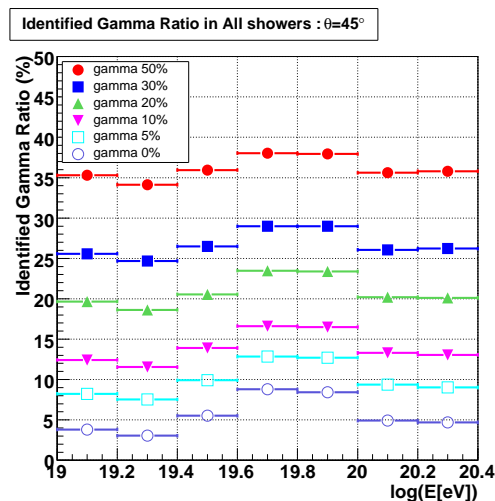


Figure 3: Ratios of showers identified as gamma-rays by NNA. Different gamma-ray fluxes between 0% and 50% are assumed as a ratio to the total flux.

come to be smaller above $10^{19.8}$ eV because UHE gamma-ray shower profiles become to be similar with ones of proton showers due to the effect of geomagnetic cascading process. Typically, misidentified ratios of 7% and 12% are seen for proton showers of 10^{20} eV and zenith angles of 45° and 60° , respectively. The stronger effect of geomagnetic cascading process for inclined gamma-rays (60°) gives a larger misidentified ratios. To estimate for an ability of NNA identification, we assumed for two components of protons and gamma-rays as primary composition with different ratios of gamma-rays between 0% and 50% in all primaries. In figure 3 ratios of showers identified as gamma-rays by NNA are shown as a function of primary energy. Each plot is also shown in cases of different gamma-ray fluxes to the total flux. Ratios of showers identified as gamma-rays for three different energy regions are shown in figure 4, as a function of assumed gamma-ray flux. If a 10% gamma-ray flux in all observed events is judged by NNA identification test, its significance of estimated gamma-ray flux depends on the statistics. More than 100 observed events in any energy regions will be required to set a $>3\sigma$ confidence by current and planned experiment.

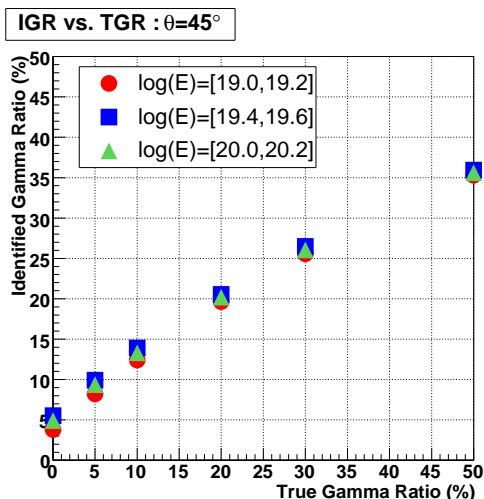


Figure 4: Relation between ratio of showers identified as gamma-rays and true gamma-ray ratio in the total flux, for three different energy regions.

The NNA is one of the powerful methods to estimate for an UHE gamma-ray flux getting behind proton primary pool. A study is in progress to increase a reliability of identification with an additional observable of the time structure of shower particles and with experimental uncertainties of X_{\max} and η .

References

- [1] K. Greisen, End to the Cosmic-Ray Spectrum?, *Physical Review Letters* 16 (1966) 748–750.
- [2] G. T. Zatsepin, V. A. Kuz'min, Upper Limit of the Spectrum of Cosmic Rays, *Soviet Journal of Experimental and Theoretical Physics Letters* 4 (1966) 78–+.
- [3] M. Takeda, N. Sakaki, K. Honda, M. Chikawa, M. Fukushima, N. Hayashida, N. Inoue, K. Kadota, F. Kakimoto, K. Kamata, S. Kawaguchi, S. Kawakami, Y. Kawasaki, N. Kawasumi, A. M. Mahrous, K. Mase, S. Mizobuchi, Y. Morizane, M. Nagano, H. Ohoka, S. Osone, M. Sasaki, M. Sasano, H. M. Shimizu, K. Shinozaki, M. Teshima, R. Torii, I. Tsushima, Y. Uchihori, T. Yamamoto, S. Yoshida, H. Yoshii, Energy determination in the Akeno Giant Air Shower Array experiment, *Astroparticle Physics* 19 (2003) 447–462.
- [4] L. Landau, I. Pomeranchuk, *Dokl. Akad. Nauk SSSR* 92 (1956) 535.
- [5] A. B. Migdal, Bremsstrahlung and Pair Production in Condensed Media at High Energies, *Physical Review* 103 (1956) 1811–1820.
- [6] B. McBreen, C. J. Lambert, *Physical Review D* 24 (1981) 2536–2538.
- [7] H. P. Vankov, N. Inoue, K. Shinozaki, Ultrahigh energy gamma rays in the geomagnetic field and atmosphere, *Physical Review D* 67 (4) (2003) 043002–+.
- [8] S. J. Sciutto, Aires: A system for air shower simulations (version 2.2.0) (1999).
URL <http://www.citebase.org/abstract?id=oai:arXiv.org:astro-ph/9911331>